Binary Level Set Methods for Dynamic Reservoir Characterization by Operator Splitting Scheme

Changhui Yao*

Department of Mathematics, Zhengzhou University, No. 100 of Science Road, Zhengzhou 450001, Henan, China

Abstract. In this paper, operator splitting scheme for dynamic reservoir characterization by binary level set method is employed. For this problem, the absolute permeability of the two-phase porous medium flow can be simulated by the constrained augmented Lagrangian optimization method with well data and seismic time-lapse data. By transforming the constrained optimization problem in an unconstrained one, the saddle point problem can be solved by Uzawas algorithms with operator splitting scheme, which is based on the essence of binary level set method. Both the simple and complicated numerical examples demonstrate that the given algorithms are stable and efficient and the absolute permeability can be satisfactorily recovered.

AMS subject classifications: 49Q10, 35R30, 65J20, 74G75

Key words: Dynamic reservoir characterization, binary level set method, operator splitting scheme, the augmented lagrangian method.

1 Introduction

We consider the conversation of mass for two-phase, incompressible, immiscible, horizontal flow in a porous medium with isotropic permeability:

$$\Phi(\mathbf{x})\frac{\partial S_o}{\partial t} - \nabla \cdot \left(\frac{\kappa(\mathbf{x})\kappa_{ro}(S_o)}{\mu_o} \nabla p_o \right) = f_o(\mathbf{x}), \tag{1.1a}$$

$$\Phi(\mathbf{x})\frac{\partial S_w}{\partial t} - \nabla \cdot \left(\frac{\kappa(\mathbf{x})\kappa_{rw}(S_w)}{\mu_w} \nabla p_w \right) = f_w(\mathbf{x}), \tag{1.1b}$$

where $(\mathbf{x}, t) \in \Omega \times [0, T]$, $\Omega \subset R^2$ is a bounded reservoir, and the subscripts o and w refer to the phases, oil and water, respectively. Also S_i denotes the saturation, μ_i

---

*Corresponding author.
Email: chyao@lsec.cc.ac.cn (C. H. Yao)

the viscosity, p_i the pressure, f_i the external volumetric flow rate and κ_{ri} is the relative permeability, where i is the fluid phase. The porosity and the absolute permeability are given by $\Phi(\mathbf{x})$ and $\kappa(\mathbf{x})$, respectively, see, e.g., [7,24].

Closuring the system is obtained through an assumption of a completely saturated medium

$$S_o + S_w = 1 \tag{1.2}$$

and an assumed known function P_c defining the capillary pressure,

$$p_o - p_w = P_c. \tag{1.3}$$

The quantities Φ, κ, κ_{ri} and P_c are all depended of the porous medium and are not accessible through direct measurements.

The considered problem is how to estimate an absolute permeability $\kappa(\mathbf{x})$, when Φ and κ_{ri} are assumed to be known, and P_c is set to zero. For recovering the permeability, we need utilize information from the wells together with seismic data. Unfortunately, we cannot get any direct information of permeability. However, through the Eqs. (1.1)-(1.3), we can use the indirect information to estimate the permeability on a coarse scale. Generally, such a problem can be called an inverse problem, or more specific referred to as a *history matching problem* [1, 27, 28]. In order to overcome the ill-posedness, regularization methods are always applied with different regularized terms.

The forward model (the solution of Eqs. (1.1)-(1.3) for a given function $\kappa(\mathbf{x})$) is solved by applying an in-house reservoir simulator. The simulator is using a standard block-centred grid with upstream weighting and Euler backwards in time discrete. Some numerical techniques can also cited in [9, 10].

In this work, we will use binary level set method [13, 17, 18] to recover the permeability. One of the essence of binary level set method is that we can constrain the solution to be a piecewise constant. And the geometries of the discontinuity of curves are allowed to be arbitrary, but with some constraint regularity achieved by a total variational regularization. For binary level set functions, the change of sign will show the discontinuity of the curves. From [14], we know that level set method can produce piecewise constant solution with a predefined number of constant levels. Practically, it can represent the sought solution with a few number of regions than the predefined number, which causes that one or more regions are empty [13]. Thus, we only need an upper bound of the number of regions in the piecewise constant solution.

This paper is based on the framework of [19]. The authors described the reservoir characterization using a binary level set approximation. They solved this problem by the augmented Lagrangian method, and used the gradient steepest descent method to get the next level set function values in their Uzawa algorithm. In [18], the authors also utilized data from wells and spatially distributed data with prior information about the sought solution to re-estimate the permeability. From the lights of work in [15, 16, 25], we can see that a better result can be obtained if operator splitting method is applied to inverse problem approximated with piecewise constant level set method without difficulties.

In our algorithm, we use the augmented Lagrangian method [5, 8] to regularize the inverse problem of dynamic reservoir characterization. Finding a proper time-step with linear search, minimizing binary level set function by operator splitting scheme and minimizing the piecewise constants by steepest gradient descent method, we can obtain good results of recovering the variation of permeability. Numerical example shows that it is more stable than the previous gradient steepest descent method because of smaller error measurements. And the computation cost is also reduced.

This paper is organized as the following: in Section 2, we describe the considered inverse problem, give the objective function and some assumptions, including data construction of reservoir modeling. In Section 3, we present a quickly recall on the framework of binary level set method and transform the optimization problem. In Section 4, we give numerical optimization formulation and deduce an operator splitting scheme. Uzawas algorithm is presented. In Section 5, we set up some preparations before our experiments. In Section 6, we give numerical experiment to show that such a Uzawas algorithm is working and we can get better results seeing from the error measurements. Computation cost can be found from the iteration step number. In Section 7, we summarize our work and give a conclusion. In Section 8, we give many thanks to the supports.

2   Contributed data and inverse problem

It is much more proper to solve the considered problem with respect to the logarithm of the permeability. Define

$$q(\mathbf{x}) = \log_{10} \kappa(\mathbf{x}), \tag{2.1}$$

we can solve this problem with respect to $q(\mathbf{x})$. It can be seen that the transformation from κ to q will not destroy the contour of the discontinuities.

Let $\mathbf{d}_{well}$ be a vector of well data, and $\mathbf{d}_{seis}$ be a vector of seismic data, and assume that all measurements have been transformed into pressures and saturations:

$$\mathbf{d}_{well} = \left\{ p_o(\mathbf{x}_{well}, t), \ S_w(\mathbf{x}_{well}, t), \ \text{for} \ i = 1, 2, \cdots, n_{well}, \ t \in [0, T] \right\}, \tag{2.2a}$$

$$\mathbf{d}_{seis} = \left\{ p_o(\mathbf{x}, \mathbf{t_j}), \ S_w(\mathbf{x}, t_j), \ \text{for} \ \mathbf{x} \in \Omega, \ j = 1, 2 \cdots, n_{seis} \right\}, \tag{2.2b}$$

where n_{well} is the number of present wells in Ω and n_{seis} is the number of seismic surveys in the time domain $[0, T]$.

From the existed experiments we know that it is much better to combine all kinds of different data into one optimization for computation and analysis. From the methods of weighting the different kinds of data in [3, 6], we apply an objective function to measure the fit of the model to the data:

$$J_{tot}(q) = J_{well}(q) + J_{seis}(q) = \frac{1}{2}(\mathbf{d}_{well} - \mathbf{m}_{well}(q))^T D_{well}^{-1}(d_{well} - \mathbf{m}_{well}(q))$$

$$+ \frac{1}{2}(\mathbf{d}_{seis} - \mathbf{m}_{seis}(q))^T D_{seis}^{-1}(d_{seis} - \mathbf{m}_{seis}(q)). \tag{2.3}$$

Here $\mathbf{m}_{well}(q)$ and $\mathbf{m}_{seis}(q)$ are the simulated values corresponding to the given measurements. These values are calculated by the forward model (Eqs. (1.1a)-(1.3)) for a given function $q(\mathbf{x})$ (or corresponding permeability function $\kappa(\mathbf{x})$). The different terms in J_{tot} are weighted by the inverse of the covariance matrices D_{well}, D_{seis}. These matrices are representing the uncertainties parts of the data and will in general not be diagonal, see [6]. The first two terms of the objective function, J_{well} and J_{seis}, will measure the misfit between the measured and the corresponding simulated data.

We utilize a regularization method to strict the solution space when reconstructing the function $q(x)$ because of highly ill-posedness. A simple piecewise constant space can be taken. From analysis shown in [12,20], we know that a total variational method can be taken to regularize $q(x)$. The actual applied regularization is

$$R(q) = \int_{\Omega} |\nabla q| dx. \tag{2.4}$$

Such a definition can control both the length of the interface and the jumps of q.

The functional to be minimized is defined as

$$F(q) = J_{tot} + \beta R(q), \tag{2.5}$$

where β is a parameter weighting $q(\mathbf{x})$. In the example q has two regions by finding the optimal function q^*, which is the solution of the following minimization problem:

$$q^* = \arg\min_{q \in Q} F(q), \tag{2.6}$$

where Q is a space of piecewise constant functions.

3 The binary level set method for the inverse problem

In the binary level set formulation, the level set functions are discontinuous, which should take the values -1 or 1 at convergence. These functions can be used to partition a domain Ω into a number of subdomains $\{\Omega_j\}$ by requiring different sign of the level set functions inside and outside the subdomains. In this way, the discontinuities of the functions will represent the boundary of the subdomains.

Assume that Ω needs to be divided into two subdomains, Ω_1 and Ω_2, such that $\Omega_1 \cap \Omega_2 = \varnothing$ and $\Omega = \bar{\Omega}_1 \cup \bar{\Omega}_2$, where $\bar{\Omega}_j$ is the closure of $\Omega_j, j = 1, 2$. A representation of this domain can be given by

$$\phi(\mathbf{x}) = 1, \quad \forall \mathbf{x} \in \Omega_1, \qquad \phi(\mathbf{x}) = -1, \quad \forall \mathbf{x} \in \Omega_2 \tag{3.1}$$

and the curve separating Ω_1 and Ω_2 is implicitly given as the discontinuity of ϕ. The properties of ϕ can be used to construct a scalar function $q(\mathbf{x})$ with distinct constant values inside the two different subdomains. If we assume that the value of $q(\mathbf{x})$ is equal to c_1 in Ω_1 and equal to c_2 in Ω_2, then q can be written as

$$q = \frac{1}{2}[c_1(\phi + 1) - c_2(\phi - 1)]. \tag{3.2}$$

Multiple level set functions can be used to represent more than two regions. Following the terminology applied in [4], N binary level set functions can be combined to produce a coefficient function with 2^N different levels. Given $\{\phi_i\}_{i=1}^N$ and $\mathbf{c} = (c_1, c_2, \cdots, c_{2^N})$, the function q can be expressed as the sum

$$q(\phi, c) = \sum_{i=1}^{2^N} c_j \psi_j(\phi), \tag{3.3}$$

where ψ_j are basis functions depended on ϕ. (3.2) is a special case of Eq. (3.3). For example, $\psi_1 = (\phi + 1)/2$ and $\psi_2 = -(\phi - 1)/2$ in Eq. (3.2).

In the following, we let $K(x) = x^2 - 1$. The level set functions are required to satisfy the constraint

$$K(\phi_i) = \phi_i^2 - 1 = 0, \quad \forall i = 1, \cdots, N. \tag{3.4}$$

This requirement will force the level set functions to take the values -1 or 1 at convergence.

After defining a constraint vector function $K(\phi) = \{K(\phi_i)\}_{i=1}^N$, the minimization problem (2.6) can be reformulated by

$$(\phi^*, c^*) = \arg \left\{ \min_{\phi, c} F(q(\phi, c)), \text{ subject to } K(\phi) = 0 \right\} \tag{3.5}$$

and the optimal function can be obtained by $q^* = q(\phi^*, c^*)$ from the Eq. (3.3).

4 Numerical optimization and operator splitting scheme

We utilize the augmented Lagrangian method to solve problem (3.5) numerically. The Lagrangian function $L(\phi, c, \lambda)$ concludes F and the constraint K:

$$L(\phi, c) = F + W, \tag{4.1}$$

where

$$F = F(q(\phi, c)), \quad W = \sum_{i=1}^N \int_\Omega \lambda_i K(\phi_i) dx + \mu_p \sum_{i=1}^N \int_\Omega |K(\phi_i)|^2 dx$$

and μ_p is a penalization parameter which usually is fixed parameter chosen a priori, or it can in some case be increased. Therefore, we usually solve the following minimization problem instead of (3.5),

$$(\phi^*, c^*) = \arg \left\{ \min_{\phi, c} L(\phi, c, \lambda) \right\}. \tag{4.2}$$

At the minimizers of $L(\cdot, \cdot, \cdot)$, we should have

$$\frac{\partial L}{\partial \phi} = \frac{\partial F}{\partial \phi} + W'(\phi) = 0, \quad \frac{\partial L}{\partial c} = 0, \quad \frac{\partial L}{\partial \lambda} = 0. \tag{4.3}$$

In order to obtain minimizers, in generally, some stable methods such as steepest gradient descent method will be used. A Uzawas type algorithm will be done like that:

Algorithm 1. Choose initial values for ϕ^0, c^0 and λ^0. For $k = 1, 2, \cdots$, do

1. Find ϕ^{k+1} such that

$$\phi^{k+1} = \phi^k - \triangle t_\phi \frac{\partial L}{\partial \phi}(\phi^k, c^k, \lambda^k). \tag{4.4}$$

2. Find $\mathbf{c^{k+1}}$ such that

$$c^{k+1} = \arg\min_c L(\phi^k, c, \lambda^k). \tag{4.5}$$

3. Update λ

$$\lambda^{k+1} = \lambda^k + \mu_p K(\phi^{k+1}). \tag{4.6}$$

4. Iterate again if necessary.

From the previous experiments [15,16,25] using piecewise constant level set method we know that one of the most difficult parts is to control the update of ϕ by minimizing $L(\phi, c^k, \lambda^k)$ with respect to ϕ. We can directly use gradient type methods with linear search to determine the optimal step length. However, for our propose, we prefer another approach. Instead of solving (4.3), we actually solve the following ordinary differential equation to the steady state

$$\phi_t + \frac{\partial L}{\partial \phi} = 0. \tag{4.7}$$

According to the operator splitting scheme [15,16,25], we can solve (4.7) in the following way: For $k = 1, 2, \cdots$, until convergence, do

$$\frac{\phi^{k+\frac{1}{2}} - \phi^k}{\tau} + \frac{\partial F}{\partial \phi}(c^k, \phi^{k+\frac{1}{2}}) = 0, \tag{4.8a}$$

$$\frac{\phi^{k+1} - \phi^{k+\frac{1}{2}}}{\tau} + W^{'}(\phi^{k+1}) = 0, \tag{4.8b}$$

where τ is a pseudo time-step. Notice that (4.8b) can be rewritten as

$$\frac{\phi - \phi^{k+\frac{1}{2}}}{\tau} + \mu_p K(\phi) K^{'}(\phi) = 0, \tag{4.9}$$

or

$$\phi - \phi^{k+\frac{1}{2}} + \alpha_2 \mu_p K(\phi) K^{'}(\phi) = 0, \tag{4.10}$$

where α_2 is a parameter that should be chosen properly. If we take $\phi^{k+1/2}$ as a constant, at every interaction, the Eq. (4.10) will be a simple type equation of $g(x) = 0$. With the help of selecting a proper α_2, in generally α_2 is larger than time-step, it is easy to get the solution ϕ using Newton iteration solution.

For solving (4.8a), notice that (4.8a) equals to

$$\min_\phi \left\{ \frac{1}{2\tau} \|\phi - \phi^k\|^2 + F \right\} = \min_\phi \left\{ \frac{1}{2}\alpha_1 \|\phi - \phi^k\|^2 + F \right\}. \tag{4.11}$$

So we can apply a gradient like method with linear search to determine the optimal step length, where $\alpha_1 = 1/\tau$ should be chosen properly.

Furthermore, in order to find the minimizer of L with respect to ϕ, the original energy function L is decomposed into two parts: $L = F + W$, which can be solved one by one, and by using operator splitting scheme, the two parts are incorporated together in a harmonious way.

The energy function L can be decomposed into two parts coincides in the nature of our model problem. In fact, our model problem consists of two stages: recovering of $q(\mathbf{x})$, which means the output-least-square, and image segmentation approximating $q(\mathbf{x})$ by a binary level set function. We just need the level set formulation in the second stage, which introduces the constraint part. So the problem is clear, and we can write our algorithm to find a minimizer of L as following:

Algorithm 2. (Uzawa algorithm and Operator splitting scheme).

Determine the number of level set function, N and the initial level set function ϕ^0 to use.

Choose time step for $\triangle t_\phi$.

Choose search interval for each $c_j, c_j \in [a_j, b_j]$.

Initialize: ϕ^0, c^0, also set $k = 0$.

1. Find ϕ^{k+1},

   (a) Get q by formula (3.3).
   (b) Compute $\phi^{k+1/2}$ by
   $$\phi^{k+\frac{1}{2}} = \phi^k - \sigma_k \frac{\partial F}{\partial \phi}(c^k, \phi^k).$$
   (c) Compute ϕ^{k+1} by (4.10) with a proper parameter α_2, or else set $\phi^{k+1} = \phi^{k+1/2}$.

2. Update c (after a fixed number of iterations because of ill-posedness). For each $c_j, j = 1, 2, \cdots, 2^N$:

   (a) Get q by formula (3.3).
   (b) Define:
   $$\alpha_{c_j}^k = \frac{\partial L}{\partial c_j}(\phi^{k+1}, c^k).$$
   (c) Define the search interval: Let $M \subset \mathcal{R}$ be all the values of $\triangle t$ such that $c_j^k - \triangle t \alpha_{c_j}^k \in [a_j, b_j]$.
   (d) Find the optimal time step: $\triangle t_{c_j} = \arg \min_{\triangle t \in M} L(\phi^{k+1}, c^k - \triangle t \alpha_{c_j}^k \mathbf{e_j})$, where e_j is the j-th unit vector.
   (e) Update the constant: $c_j^{k+1} = c_j^k - \triangle t \alpha_{c_j}^k$.

3. Iterate again if necessary.
   $$k := k + 1.$$

Derived from the ill-posedness of our model problem and q updated implicitly using the most recently calculated values of ϕ and $\mathbf{c}$, in this algorithm, we can not use Step 2 and Step 3 in every step. Otherwise, the algorithm will be unstable if ϕ and $\mathbf{c}$ are updated too often. In principle we can have run Step 1 to convergence before doing other steps. Therefore, we can update $\mathbf{c}$ and λ after a fixed number of iterations. To further stabilize Step 2, we have applied a predefined search interval $[a_j, b_j]$ for each constant such that there will be no risk of producing values completely out of range.

We have found that it is difficult to find any suitable stopping criterion which stop the iterations before the solution is strictly piecewise constant. In this work, we will run the algorithm to a fixed number of iterations.

5   Setup for numerical tests

In this section, we will present a complicated example to demonstrate the analysis of our model problem and the efficiency of the given algorithm. The utilized example is synthetic case where the true permeability field consists of two distinct permeability values. And in this case it is sufficient with one level set function to represent the field. The considered reservoir is square and horizontal with constant thickness and non-flow outer boundary. Except for the absolute permeability, the fluid and rock properties are held fixed through the simulations. And in the field we have one injector positioned in the lower left corner and one producer positioned in the upper right corner.

The relative permeability functions are defined by Corey models:

$$\kappa_{rw} = \hat{\kappa}_{rw} \Big(\frac{S_w - S_{wr}}{1 - S_{wr} - S_{or}} \Big)^{e_w}, \quad \kappa_{ro} = \hat{\kappa}_{ro} \Big(\frac{S_o - S_{or}}{1 - S_{or} - S_{wr}} \Big)^{e_o},$$

where the Corey exponents, e_w and e_o, the residual saturations, S_{wr} and S_{wo}, and the endpoint permeability, $\hat{\kappa}_{rw}$ and $\hat{\kappa}_{ro}$, are assumed known. The numerical values for these properties are, together with the rest of the properties for the simulations, listed in Table 1.

The forward model (1.1)-(1.3) is solved by applying an in-house reservoir simulator. In this simulator the equation error is minimized by applying Newton iterations, and the linear solver of choice is GMRES. The gradient $\partial F / \partial q$ is solved from the solution of the adjoint system of equations [22].

In numerical experiments, it is desirable to replace $\tilde{\phi}_i$ by a smoothed approximation. The chosen approximation is

$$\tilde{\phi}_i \approx \frac{\phi_i}{\sqrt{\phi^2 + \epsilon}}, \tag{5.1}$$

where ϵ is a small positive number which has to be chosen.

For each reference permeability field we calculate the true values of saturation (S_w) and pressure (p_o) for the applied timesteps on the given grid. Thereafter synthetic measurements are constructed by adding noise to the calculated true values.

Table 1: Numerical values for simulations.

Reservoir dimensions:	$1000 \times 1000 \times 40$ meter
Simulation grid:	$16 \times 16 \times 1$ cells
Porosity:	0.2
Viscosity:	$\mu_w = 0.5 \times 10^{-3}$Pa·s, $\mu_o = 0.5 \times 10^{-3}$Pa·s
Endpoint relative permeability:	$\hat{\kappa}_{rw}$=0.1, $\hat{\kappa}_{ro}$=0.1
Residual saturations:	$S_{rw} = 0.2$, $S_{or}^* = 0.2$
Corey exponents:	$e_w = 1.5$, $e_o = 2.5$
Initial saturations:	$S_w = 0.2$, $S_o = 0.8$
Capillary pressure function:	$P_c(S_w) \equiv 0$KPa
Injector rate:	8% of total pore volume per year
Production rate:	constant BHP= 200.0bar
Number of timesteps:	192
Total production time:	3000 days
Number of seismic surveys:	16 (i.e., approximately every 6 months)

Table 2: The standard derivations.

	Well data	Seismic data
Pressure	$\sigma_{p,well} = 1.0$bar	$\sigma_{p,seis} = 2.5$bar
Saturation	$\sigma_{S,well} = 0.025$	$\sigma_{S,seis} = 0.050$

The noise is assumed to be uncorrelated Gaussian noise with zero mean. In Table 2 the standard derivations which give the amount of added noise are listed. Notice that the uncertainties are larger for the seismic measurements than for the measurements in the wells. When calculating $J_{tot}(q)$ we use the correct uncertainties, according to the added noise, for constructing D_{well} and D_{seis}.

The penalization parameter μ_p is increased slowly through the iterations. If k is the number of iteration, $\mu_p = 0.05 \times 1.01^k$ up till it reaches an upper bound (equal to 4) where we keep it fixed. Regarding the regularization parameter β, we have for each example first tried with a value of 5×10^{-3}. If this causes large oscillations in the solution, then the weight on the regularization is increased and a new optimization is preformed. The value of ε used to calculate $\tilde{\phi}$ is initially equal to $0, 1$, and is decreased by a factor of 0.98 until it reaches a lower bound equal 10^{-7}. The c_j-values are updated each 10th iteration. Also we can choose a larger parameter α_2 than time-step in (4.10) in order to control the convergence by adding constraint function and penalty function. Here, we take $\alpha_2 = 0.1$.

For each test case we start with ϕ^0 in the entire domain except in the cells where we have wells. In the cells with a penetrating well, we assume that the approximating the permeability value is known. The value of ϕ is therefore fixed equal to its correction value (1 or -1 dependent of the initial **c**-values) in the cells.

For each of the constant values we define an interval $[a_j, b_j]$ within c_j can be estimated. The length of this interval will be associate to the *prior* uncertainty of the permeability value for corresponding domain. Because there are abilities for direct measurements of the permeability in the wells, we have applied a lower uncertainty for c_j in the regions where there is at least one well present, than for the regions with

no wells. For the studied case we have applied interval $[a_j, b_j]$ with length equal 50% (no wells) and 30% (wells) of the difference between the two true values of q. The center of the intervals are chosen equal to the true values. For example, if we assume the following: c_1 and c_2 are the true values, the domain corresponding to c_1 has no wells present and there are one or more wells penetrating a region with permeability approximately equal to c_2. Then the bounds will be

$$a_1 = c_1 - 0.25 \cdot |c_2 - c_1|, \quad b_1 = c_1 + 0.25 \cdot |c_2 - c_1|$$

and

$$a_2 = c_2 - 0.15 \cdot |c_2 - c_1|, \quad b_2 = c_2 + 0.15 \cdot |c_2 - c_1|.$$

In this paper, we start with initial c_j-values on the lower and upper bound of the two intervals. We use the lower bound for the smallest c_j values and the upper bound for the highest c_j value, that is, if $c_1 < c_2$, then $c_1^0 = a_1$ and $c_2^0 = b_2$. Other approaches for choosing the initial values are also possible.

The algorithm is stopped after 1000 iterations if ϕ^k and $\mathbf{c}^k$ have not converged, in the sense of stopped changing, before this.

For each considered example, we have plotted measurements of the errors and the convergence. One of the measurements is the equation error. We define $e_o(q, p_o, S_w)$ and $e_w(q, p_o, S_w)$ to be the equation residual for (1.1a) and (1.1b), respectively, and let the equation error

$$E(q, p_o, S_w) = \sum_{i=o,w} \|e_i(q, p_o, S_w)\|_{L_2(\Omega \times [0,T])}. \tag{5.2}$$

Since Eqs. (1.1a) and (1.1b) are solved exactly, in the forward model, the residual $E(q^k, m(q^k))$ should be zero or below a numerical error bound.

To measure the data fit we plot RMS values of J, J_{well} and J_{seis} versus the iteration number. The RMS value of a function J_α is defined as $\sqrt{2J_\alpha/n_\alpha}$, where n_α is the number of measurements included in J_α and $\alpha = tot, well$ or $seis$.

Other measurements applied to check the convergence are $\|K(\phi^k)\|_{L_2}$ and $\|K(\tilde{\phi}^k)\|_{L_2}$. The difference between these two measurements is that the first one indicates how fast ϕ^k reaches the convergence values -1 and 1, and the second one is a measure of how close $\hat{q}^k$ is from being piecewise constant with only two levels.

6 Numerical examples

Example 6.1. *S*-shape Channel.

In this example, we take a *S*-shape channel as a true field with high permeability from the injector to the producer. From the discussion in [18,19] we know that we can use *one level set* function to identify three distinct piecewise constant region since two of the regions have the same constant value. And also we know the authors gave some
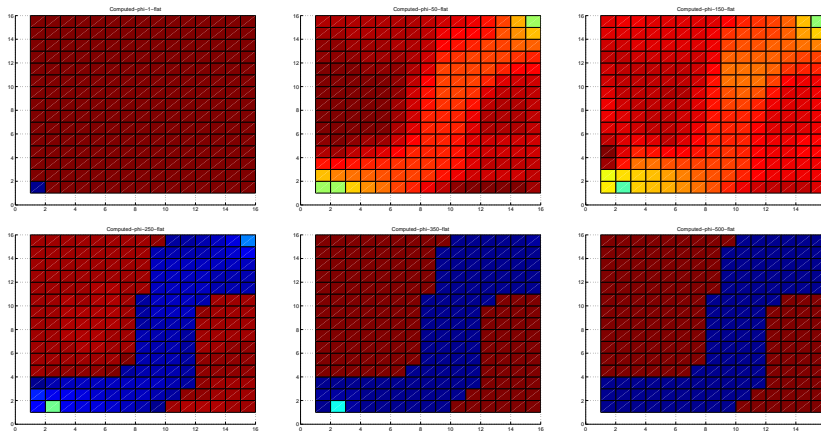
Figure 1: Show ϕ at 1-th, 50-th, 150-th, 250-th,350-th,500-th iteration using Algorithm 2.
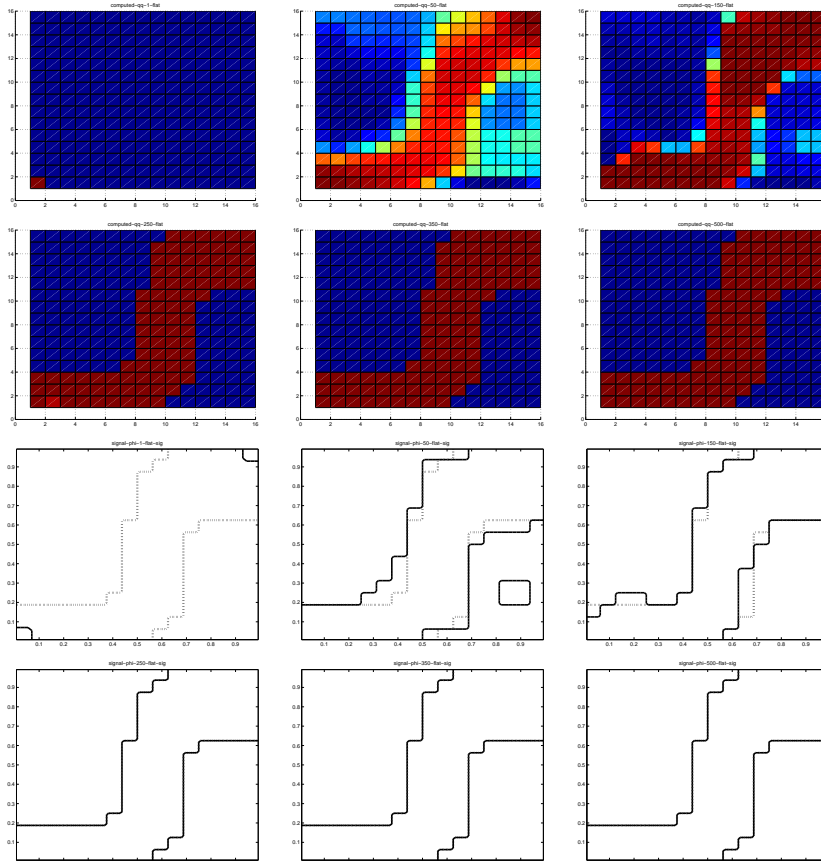

Figure 2: Show q^k and the signal change of q^k at 1-th, 50-th,150-th,250-th,350-th,500-th iteration using Algorithm 2, respectively. In the upper two rows, q^k is given. In the lower two rows, the solid line shows the discontinuities of the recovered q^k and the dotted line shows the true discontinuity of q.

results by using Algorithm 1. Here we will not recite all the results made by them and only give the comparison with the two algorithms.

Firstly, Fig. 1 gives the convergence procedure of level set function ϕ. From this figure, we can see that Algorithm 2 will give a good convergence for ϕ after 250-th iteration. Fig. 2 can also make a similar conclusion from the signal change of q^k. Both the two figures show that there is few error when we recover q^k by using Algorithm 2 after 250-th iteration. However, there were 1.17% errors on the same considered field [19] (Fig. 4h) and 0.39% errors after modifying the Algorithm 1 in [19]. Fig. 3 presents a comparison of signal change using Algorithm 2 and 1 in the left two figures. The error rate is 0 and 0.39%, respectively. The right three figures show the comparison the exact q with the computed q. In Fig. 4, we put our issues on the comparison the error measurements with the two algorithms. The red line is plotted by the results obtained by Algorithm 1 and the black line is plotted by the results obtained by Algorithm 2. From this figure we know that the recovered permeability q^k has less error using Algorithm 2 than Algorithm 1, though the piecewise constant values and RMS has the similar errors, respectively. Fig. 5 show the measures of convergence of constraint functions $K(\phi), K(\tilde{\phi})$. From this comparison we know that the modified $\tilde{\phi}$ will have much more stability and less oscillation. In Fig. 6, we give the comparison of $E(q^{k+1}, m(q^k))$ using Algorithm 2 and Algorithm 1. The red curve is an average of $E(q^{k+1}, m(q^k))$ for the last 15 iterations. The curves indicate convergence after 250 iterations for Algorithm 2 and after 400 iterations for Algorithm 1. In Fig. 7, using Algorithm 1 and Algorithm 2, pressure and saturation are plotted at the end of simulation (3000 days), $\mathbf{c} = (0, 0.3)$ and injection rate is equal to 8% of the total pore volume per year. Here, the complete field is flooded by water at the simulation.
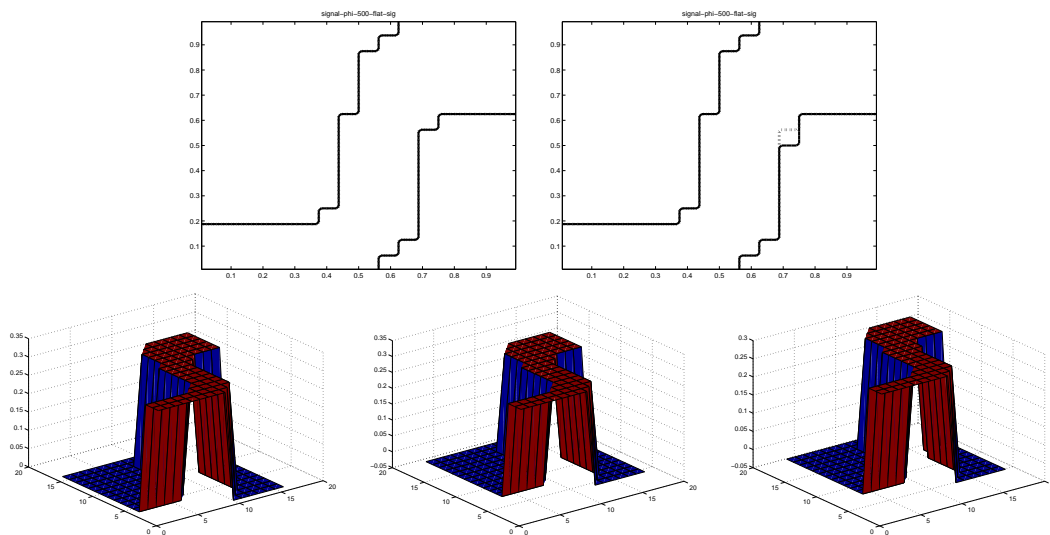

Figure 3: The left two figures show sign change of ϕ compared Algorithm 2 with Algorithm 1. The error rate is 0 and 0.39%, respectively. The right three figures show the comparison the exact q with the computed q using Algorithm 2 and Algorithm 1, respectively.
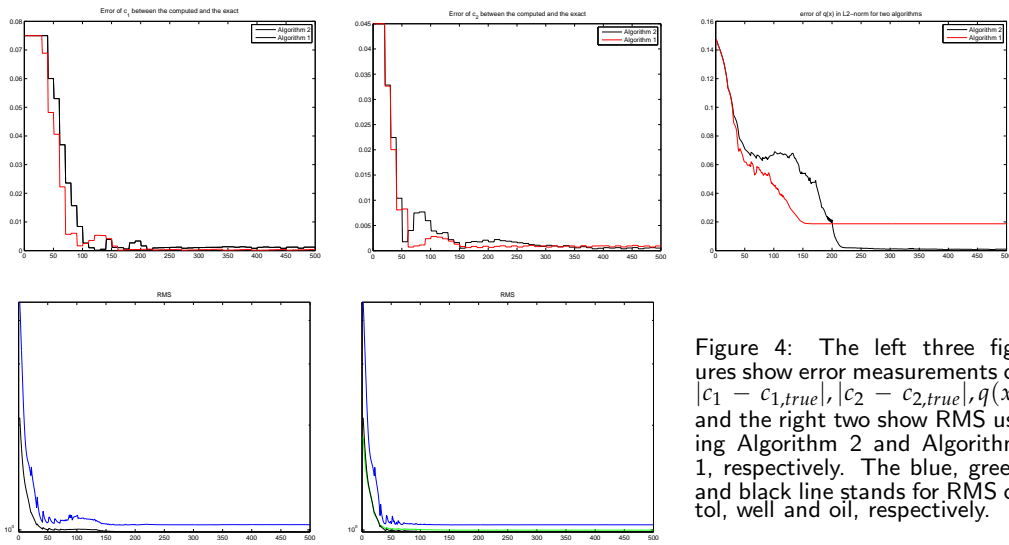
Figure 4: The left three figures show error measurements of $|c_1 - c_{1,true}|, |c_2 - c_{2,true}|, q(x)$ and the right two show RMS using Algorithm 2 and Algorithm 1, respectively. The blue, green and black line stands for RMS of tol, well and oil, respectively.
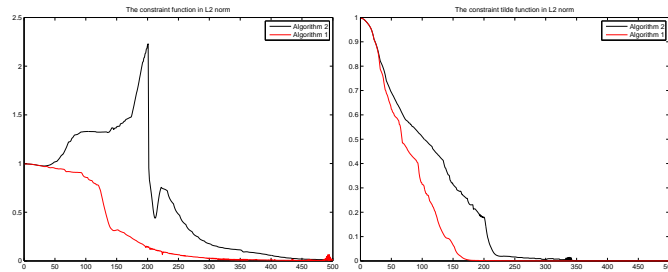

Figure 5: Show the comparison $\|K(\phi)\|_{L^2}$ and $\|K(\tilde{\phi})\|_{L^2}$ using Algorithm 2 and Algorithm 1.
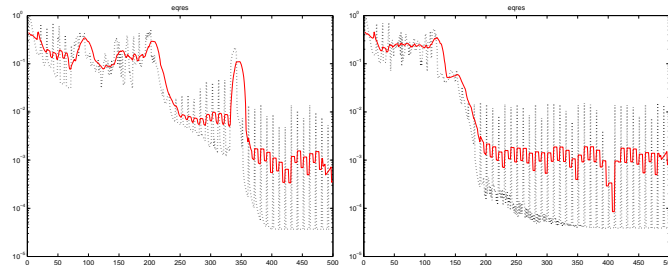

Figure 6: $E(q^{k+1}, m(q^k))$ with Algorithm 2 and 1. The red curve is an average of $E(q^{k+1}, m(q^k))$ for the last 15 iterations.

Example 6.2. Complicated field-crossing channel.

In this example, we demonstrate a complicated field in [18] where two channels are crossing each other. And we also assume that the two channels have the same permeability value and they produce a connected region with high permeability from the injector to the producer.

First, we show the convergence procedure of level set function ϕ^k using Algorithm 2 in Fig. 8. We can see that level set function ϕ^k has almost converged to two piecewise
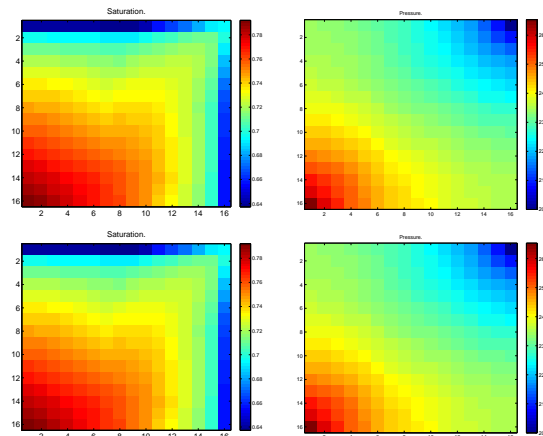
Figure 7: The left two figures are saturation run by Algorithm 2 at the end of simulation. The right two figures are pressure run by Algorithm 1 at the end of simulation.
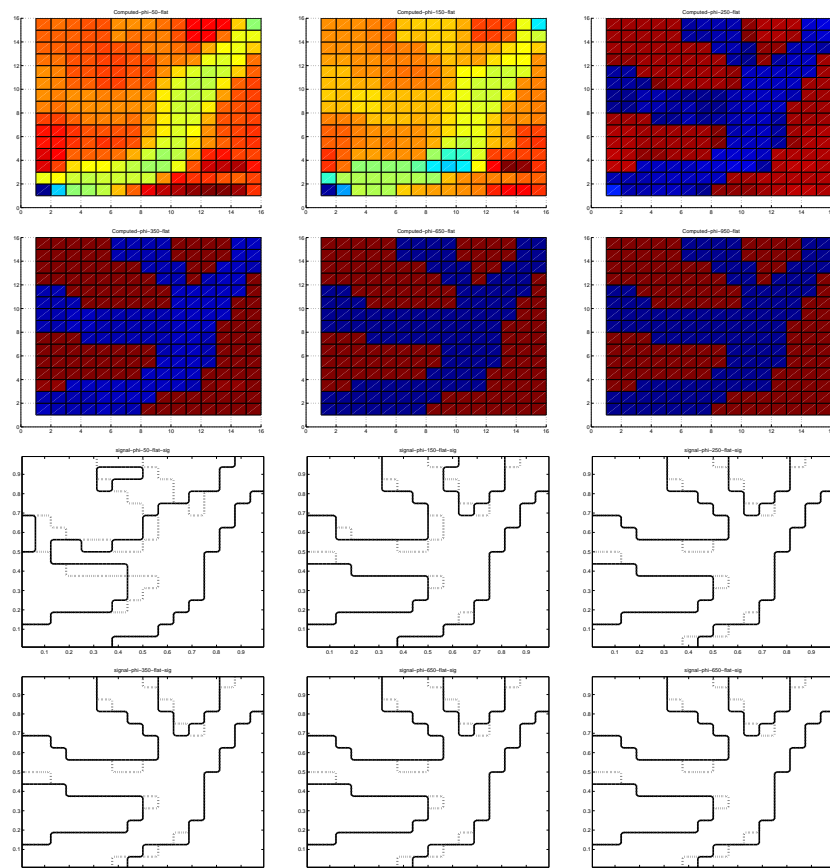

Figure 8: In the upper two rows, Show ϕ at 50-th, 150-th,250-th,350-th,650-th,1000-th iteration using Algorithm 2. In the lower two rows, the solid line shows the discontinuities of the recovered q and the dotted line shows the true discontinuity of ϕ.
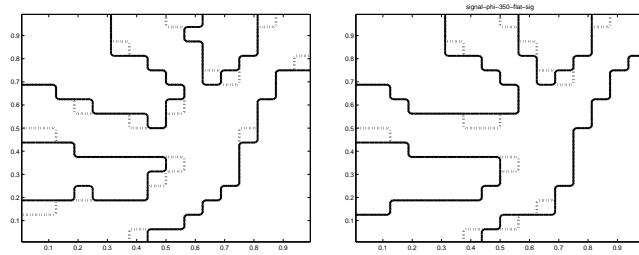
Figure 9: Sign change of q with respect to Algorithm 1 and Algorithm 2. And the error rate is 7.42% and 5.46%, respectively.
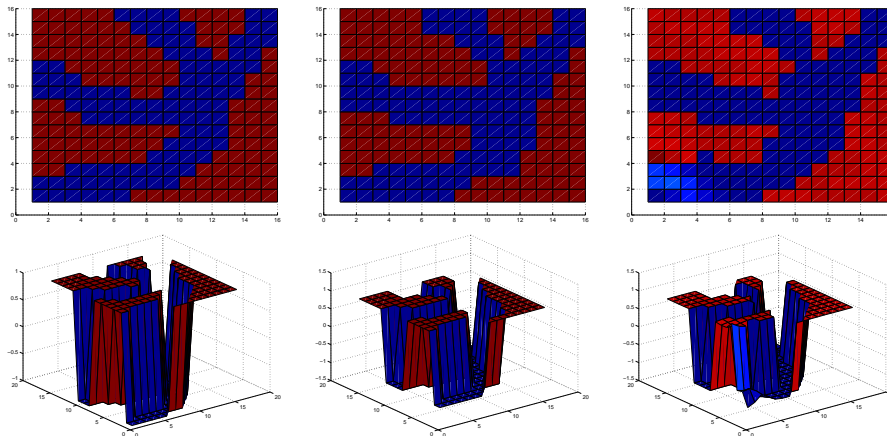
Figure 10: The comparison with exact ϕ and computed ϕ using Algorithm 2 and Algorithm 1.
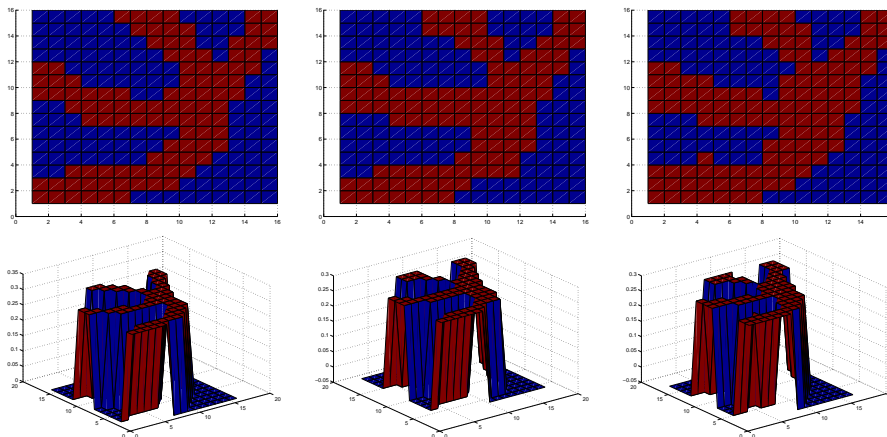
Figure 11: The comparison with exact q and computed q using Algorithm 2 and Algorithm 1.

constant after 350-th iteration. In Fig. 9, the result (error rate 5.46%), obtained by Algorithm 2, not only has less error than that obtained by Algorithm 1, error rate is 7.42%, but also it has less computation cost compared with at lest 500 iterations in [19]. Fig. 10 and Fig. 11 show the comparison ϕ and q respectively obtained by Algorithm 1 and Algorithm 2.
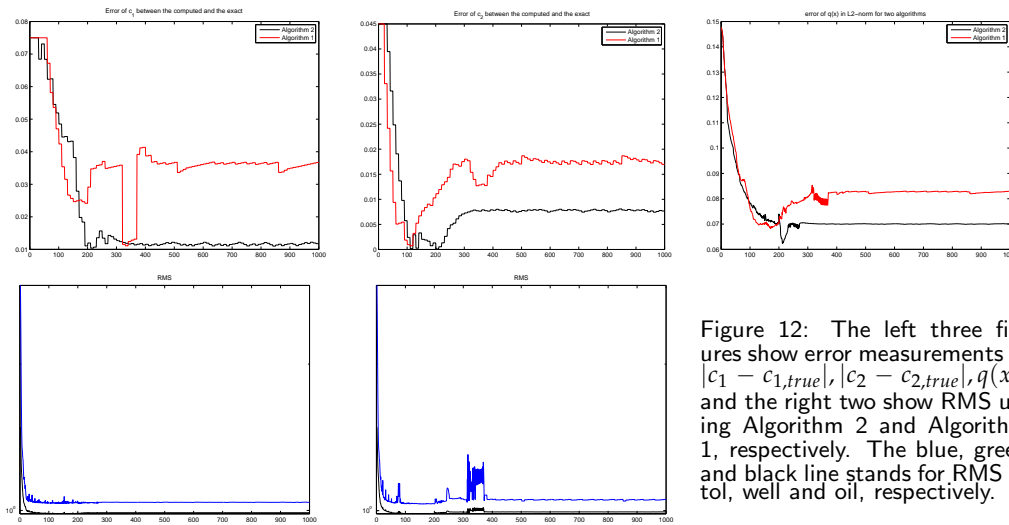
Figure 12: The left three figures show error measurements of $|c_1 - c_{1,true}|, |c_2 - c_{2,true}|, q(x)$, and the right two show RMS using Algorithm 2 and Algorithm 1, respectively. The blue, green and black line stands for RMS of tol, well and oil, respectively.
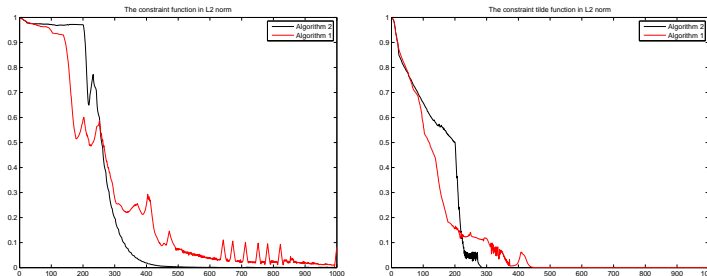

Figure 13: Comparison $\|K(\phi)\|_{L^2}$ and $\|K(\tilde{\phi})\|_{L^2}$ using Algorithm 2 and Algorithm 1. The red line shows the error computed by Algorithm 1 and the black line shows the error computed by Algorithm 2.
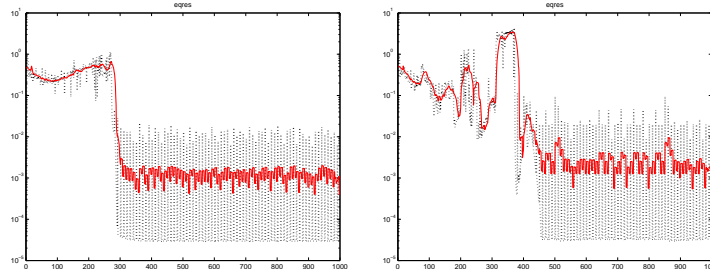

Figure 14: $E(q^{k+1}, m(q^k))$ is the norm of the equations residual, where the red curve is an average of $E(q^{k+1}, m(q^k))$ for the last 15 iterations.

Fig. 12 show the error measurements for the piecewise constant values **c**, q and *RMS*. The five subfigures tell us that Algorithm 2 can cause much less error and oscillation. Fig. 13 show that the L^2 norm of the modified level set function $\tilde{\phi}$ defined by (5.1). Obviously, the right subfigure has less oscillation.

Fig. 14 shows the equations residual of $E(q^{k+1}, m(q^k))$. The red curve is an average of $E(q^{k+1}, m(q^k))$ for the last 15 iterations. The curves indicate convergence after 350-th
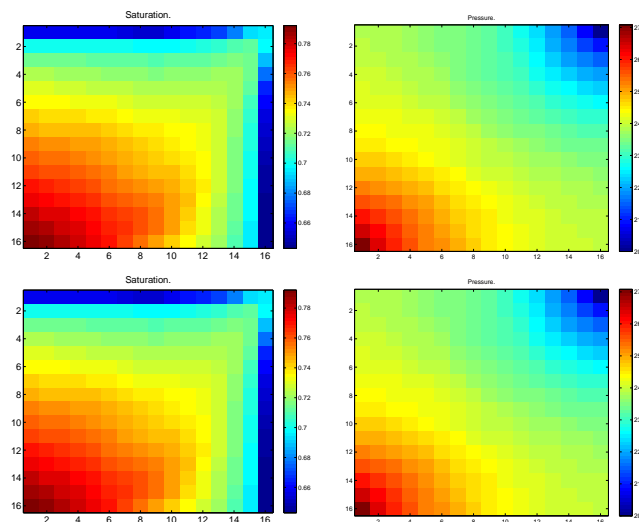
Figure 15: The left two figures are saturation obtained by Algorithm 2 at the end of simulation. The right two figures are pressure obtained by Algorithm 1 at the end of simulation.

iteration for Algorithm 2 and after 500-th iteration for Algorithm 1. In the last figures, we give the pressure and saturation. They are plotted at the end of simulation (3000 days), $\mathbf{c} = (0, 0.3)$ and injection rate is equal to 8% of the total pore volume per year. Here, the complete field is flooded by water at the simulation.

7   Conclusions

We have applied a binary level set formulation for solving inverse two-phase porous media flow problems. Both well data and seismic time-lapse data are used in the optimization process. The method is searching a piecewise constant solution of the inverse problem and it is regularized by a total variational norm. In this process, the permeability estimation can be solved by the augmented Lagrangian optimization method. After adding the constraint function to the augmented Lagrangian optimization function, the saddle point can be found by operator splitting scheme based on the essence of binary level set method.

The numerical test focuses on piecewise constant permeability fields with two different constant level. The example shows that the method can recover the main structures of permeability even with rather complicated system of channels. The figures demonstrate that the given algorithm is stable and efficient.

Acknowledgments

References

[1] S. I. AANONSEN AND D. EYDINOV, *A multiscale method for distributed parameter estimation with application to reservoir history matching*, Comput. Geosci., 10(1) (2006), pp. 97–117.

[2] Z.-Z. BAI, Y.-M. HUANG, M. K. NG AND X. YANG, *Preconditioned iterative methods for algebraic systems from multiplicative half-quadratic regularization image restorations*, Numer. Math. Theor. Meth. Appl., 3 (2010), pp. 461–474.

[3] T. BARKVE A. COMINELLI O. GOSSELIN, M. KOLASINSKI, H. REME, S. I. AANONSEN, AND I. AAVATSMARK, *Effect of scale dependent data correlation in an integrated history matching loop combining production data and 4d seismeic data*, Technical report, presented at the SPE Reservoir Simulation Symposium held in Houston, Texas, Feb.2003.

[4] T. CHAN AND L. A. VESE, *Active contours without edges*, IEEE Tran. image Proc., 10 (2001), pp. 266–277.

[5] T. F. CHAN AND X.-C. TAI, *Augmented lagrangian and total variation methods for recovering discontinuous coefficients from elliptic equations*, in M. Bristeau, G. Etgen, W. Fitzgibbon, J. L. Lions, J. Periaux and M. F. Wheeler, editors, Computational Science for the 21st Century, pp. 597–607, John Wiley & Sons, 1997.

[6] O. GOSSELIN, I. AAVATSMARK, S. IAANONSEN, A. COMINELLI AND T. BARKVE, *Integrationn of 4d data in the history match loop by investigating scale dependent correlations in the acustic impedence cube*, Technical report, Proc. 8th European Conference on Mathematics of Oil Recovery, Freiberg, German, 2002.

[7] W. GUAN AND H. S. HU, *The parameter averaging technique in finite-difference modeling of elastic waves in combined structures with solid, fluid and porous subregions*, Commun. Comput. Phys., 10 (2011), pp. 695–715.

[8] K. ITO AND K. KUNISCH, *The augmented Lagrangian method for parameter estimation in elliptic systems*, SIAM J. Control Optim., 28 (1990), pp. 113–136.

[9] K. ITO, Z.-L. LI AND Z. QIAO, *The sensitivity analysis for the flow past obstacles problem with respect to the Reynolds number*, Adv. Appl. Math. Mech., 4 (2012), pp. 21–35.

[10] K. ITO AND Z. QIAO, *A high order compact MAC finite difference scheme for the stokes equations: augmented variable approach*, J. Comput. Phys., 227(17) (2008), pp. 8177–8190.

[11] F. LI AND M. K. NG, *Kernel density estimation based multiphase fuzzy region competition method for texture image segmentation*, Commun. Comput. Phys., 8 (2010), pp. 623–641.

[12] H.-W. LI AND X.-C. TAI, *Piecewise constant level set method for multiphase motion*, Int. J. Numer. Anal. Model., 4(2) (2007), pp. 291–305.

[13] J. LIE, M. LYSAKER AND X.-C. TAI, *A binary level set model and some applications for Mumford-Shah image segmentation*, IEEE Trans. Image Proc., 15(4) (2006), pp. 1171–1181.

[14] J. LIE, M. LYSAKER AND X.-C. TAI, *A variant of the level set method and applications to image segmentation*, Math. Comput., 75(255) (2006), pp. 1155–1174.

[15] T. LU, P. NEITTAANMÄKI AND X.-C. TAI, *A parallel splitting up method and its application to Navier-Stokes equations*, Appl. Math. Lett., 4(2) (1991), pp. 25–29.

[16] T. LU, P. NEITTAANMÄKI AND X.-C. TAI, *A parallel splitting-up method for partial differential equations and its applications to Navier-Stokes equations*, RAIRO Modél. Math. Anal. Numér., 26(6) (1992), pp. 673–708.

[17] L. K. NIELSEN, H.-W. LI, X.-C. TAI, S. I. AANONSEN AND M. ESPEDAL, *Reservoir description using a binary level set model*, Comput. Vis. Sci., 13(1) (2009), pp. 41–58.

[18] L. K. NIELSEN, X.-C. TAI, S. I. AANONSEN AND M. ESPEDAL, *Identifying reservoir facies using a binary level method*, SPE, 2007, accepted.

[19] L. K. NIELSEN, X.-C. TAI, S. I. AANONSEN AND M. ESPEDAL, *Reservoir decription using a binary level set model*, CAM-report-05-50, UCLA, Applied Mathematics, 2005.

[20] L. K. NIELSEN, X.-C. TAI, SIGURD IVAR AANONSEN AND MAGNE ESPEDAL, *A binary level set model for elliptic inverse problems with discontinuous coefficients*, Int. J. Numer. Anal. Model., 4(1) (2007), pp. 74–99.

[21] L. RADA AND K. CHEN, *A new variational model with dual level set functions for selective segmentation*, Commun. Comput. Phys., 12 (2012), pp. 261–283.

[22] A. C. REYNOLDS, R. LI AND D. S. OLIVER, *History matching of three-phase flow production data*, SPE Journal, 8(4), December 2003.

[23] K. REN, *Recent developments in numerical techniques for transport-based medical imaging methods*, Commun. Comput. Phys., 8 (2010), pp. 1–50.

[24] P. SONG AND S. Y. SUN, *Contaminant flow and transport simulation in cracked porous media using locally conservative schemes*, Adv. Appl. Math. Mech., 4 (2012), pp. 389–421.

[25] X.-C. TAI, O. CHRISTIANSEN, P. LIN AND I. SKJAELAAEN, *A remark on the MBO scheme and some piecewise constant level set methods*, CAM-report-05-24, UCLA, Applied Mathematics, 2005.

[26] L.-L. WANG AND Y. GU, *Efficient dual algorithms for image segmentation using TV-Allen-Cahn type models*, Commun. Comput. Phys., 9 (2011), pp. 859–877.

[27] S.-G. WANG, G.-Z. ZHAO, L.-B. XU, D. GUO AND S.-Y. SUN, *Optimization for automatic history matching*, Int. J. Numer. Anal. Model., 2 (2005), pp. 131–137.

[28] J.-P. ZHU AND Y. M. CHEN, *Multilevel grid method for history matching multidimensional multiphase reservoir models*, Appl. Numer. Math., 10(2) (1992), pp. 159–174.